Modeling and Stability Analysis of Grid-Connected Inverters with Different LCL Filter Parameters

David Carballo, Edgar Escala and Juan Carlos Balda
Department of Electrical Engineering
University of Arkansas at Fayetteville
Fayetteville, Arkansas, USA
email: dmcarbal@uark.edu, eaescala@uark.edu, jbalda@uark.edu

***Abstract*— Microgrid are gaining popularity due to several advantages like potential for fuel savings and resiliency in case of grid catastrophic failures. In a microgrid, many energy sources like wind and solar farms are connected to the grid through inverters with different power ratings and LCL filter parameters. The inverters incorporated in these systems might have a different frequency response and stability ranges than those inverters with identical LCL filter values. This paper establishes the model and analyzes the stability of a system with multiple paralleled- and grid-connected inverters with different LCL filter paramenters using the grid-side currents as feedback signals. The analysis results showed that a method similar to the interactive and common current analysis technique used on inverters with identical LCL filters can be implemented on a system with different LCL filers to calculate the maximum values of the inverters' current controller gains without having to derive the complicated equations of the MIMO system.**

Keywords*— Grid-connected inverters, LCL filters, multiparallel inverters, stability anaylsis, current control.

I. INTRODUCTION

The growing demand for renewable energy sources, such as solar energy, wind energy, and even energy storage has led to higher penetration of distributed energy resources (DERs) into power systems during the past years. As a result, the design of controllers for grid-connected inverters interfacing DERs and the electric grid has become a crucial task. In renewable power plants, hundreds of inverters operate in parallel to expand the total generation capacity [1]. These paralleled inverters are usually connected to the grid through LCL filters which tend to aggravate the system resonance and instability issues due to coupling produced by the grid impedance and converter's current controller dynamic interactions [2].

These instabilities problems due to the coupling of the inverters LCL filters have been studied thoroughly in the literature. Usually in these studies, the inverters are assumed to have identical LCL filter parameters in order to reduce the complexity of the analysis [3-5]. However, a wide variety of energy sources are incorporated in a microgrid; thus, LCL filters with different parameters and power ratings are connected to the point of common coupling (PCC). Consequently, these inverters have different system responses than those inverters with identical LCL filter values. The authors of [6] presented an analysis on the relationship between the resonant frequency and the different numbers of parallel inverters, the LCL filter parameters as well as the inverter's composition ratios. However, an analysis of the system regarding the stability ranges for the current controllers' proportional gain was not performed. The work presented in this paper aims to model and analyze multiple grid-connected inverters with different LCL filter parameters with the ultimate goal of simplifying the stability analysis to determine the proportional gain stability ranges of the inverters.

This paper is organized as follows: Section II addresses an overview of the mathematical modeling of the grid-side currents, Section III evaluates the system stability, Section IV illustrates a method to reduce the complexity of the system's stability analysis, Section V analyzes simulation results, and Section VI provides the main conclusions.

II. MODELING OF PARALLELED INVERTERS

A. Grid-Side Current − Mathematical Modeling

Two grid-connected inverters with different LCL filters are initially considered to decrease the complexity of the analyzed system. The parallel operation of these inverters is illustrated in Fig. 1, where Z_{11}, Z_{21} and Z_{31} are the s-domain impedances of the LCL filter for the first inverter, Z_{12}, Z_{22} and Z_{32} are the LCL filter impedances of the second inverter, and Z_g is the grid impedance. In this paper, the equivalent series resistance (ESR) of the components is neglected in order to consider the worst-case stability scenario where the LCL filter resonance is completely undamped. The dynamics of the system from Fig. 1 can be described using multivariable control theory as:

$$\mathbf{i_{on}} = \mathbf{G(s)} \cdot \mathbf{v_{on}} \Leftrightarrow \begin{bmatrix} i_{o1} \\ i_{o2} \end{bmatrix}, = \begin{bmatrix} G_{11} & G_{12} \\ G_{21} & G_{22} \end{bmatrix} \cdot \begin{bmatrix} v_{o1} \\ v_{o2} \end{bmatrix}, \quad (1)$$

where $\mathbf{i_{on}}$ is the output vector of the grid-side current, $\boldsymbol{v}_{\mathbf{on}}$ the input vector of the inverters voltages and **G(s)** the transfer function matrix that provides the relationship between the grid-side current with respect to the inverter voltages. The diagonal terms of **G(s)** are the influence of an inverter current (e.g., i_{o1}) due to its own inverter voltage (e.g., v_{o1}), and the non-diagonal terms are the influence of an inverter current (e.g., i_{o1}) due to another inverter voltage (e.g., v_{o2}).

978-1-5386-6705-7/18/$31.00 ©2018 IEEE

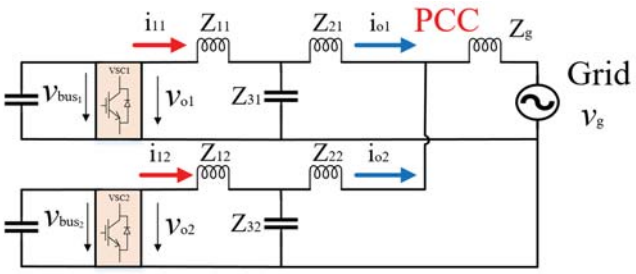

Fig. 1. Schematic of multiple grid-connected inverters with different LCL filter parameters.

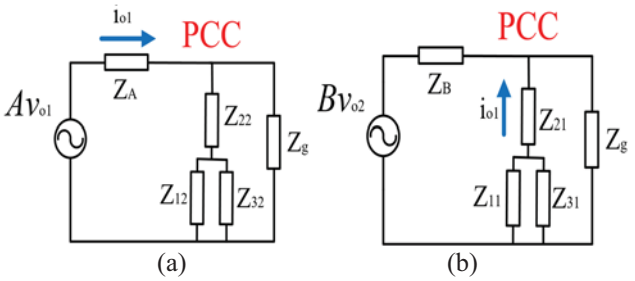

Fig. 2. Auxiliary circuit of two parallel inverters with different LCL filters parameters provided that (a) all voltage sources except v_{o1} are zero, (b) all voltage sources except v_{o2} are zero.

Similar to the case with identical LCL filters, the grid inductance causes coupling between the two inverters and, thus, the non-diagonal terms in the **G(s)** matrix are non-zero. Moreover, unlike identical LCL filters, each term in the **G(s)** matrix differ from one another, which increases the complexity when analyzing the system.

Using the principle of superposition to remove the influence of the grid and the other inverter voltages, each element in the **G(s)** matrix can be obtained. For instance, the diagonal element G_{11} is derived by removing all voltage sources except v_{o1} while the non-diagonal element G_{12} is obtained by removing all voltage sources except v_{o2}. Using source transformation, the auxiliary circuits of Figs. 2(a) and 2(b) are derived from Fig. 1 where the equivalent impedances and coefficient for the voltage sources can be written as:

$$A = \frac{Z_{31}}{Z_{11}+Z_{31}}, \qquad B = \frac{Z_{32}}{Z_{12}+Z_{32}}, \tag{2}$$

$$Z_A = \frac{Z_{11}Z_{21}+Z_{11}Z_{31}+Z_{21}Z_{31}}{Z_{11}+Z_{31}}, \quad Z_B = \frac{Z_{12}Z_{22}+Z_{12}Z_{32}+Z_{22}Z_{32}}{Z_{12}+Z_{32}} \tag{3}$$

From the auxiliary circuit in Fig. 2(a), G_{11} is obtained as:

$$G_{11} = \frac{i_{o1}}{v_{o1}} = \frac{Z_{31}}{(Z_{11}+Z_{31})(Z_A + \dfrac{Z_g Z_B}{(Z_g+Z_B)})}. \tag{4}$$

Likewise, G_{12} is derived from Fig. 2(b) as:

$$G_{12} = \frac{i_{o1}}{v_{o2}} = -\frac{Z_{32}Z_g}{(Z_{12}+Z_{32})(Z_A + \dfrac{Z_g Z_B}{(Z_g+Z_B)})(Z_g+Z_B)}. \tag{5}$$

The remaining elements of the **G(s)** matrix are derived in a similar manner and their expressions are given in the Appendix.

B. Selection of LCL Filter Parameters

The authors of [7] presented a systematic design methodology for selecting the parameters of an LCL filter for grid-connected applications. The inverter-side inductance, for example, is given by:

$$L_1 = \frac{V_{DC}V_{ph}}{0.2 f_{sw} P_n \sqrt{2}}. \tag{6}$$

where V_{DC} is the DC link voltage of the inverter, V_{ph} the phase voltage, f_{sw} the switching frequency, and P_n the nominal power.

Expression (6) shows that the value of the inductor is inversely proportional to the nominal power of the inverter. Thus, any change to the nominal power of the inverter if the other inverter parameters remain the same will be inversely reflected to the value of the inverter-side inductance. The equation for the grid-side inductor shows the same inversely proportional relation to the nominal power [7]. However, the filter capacitor is determined as a 5 percent of its base impedance given by:

$$C_f = 0.05\frac{P_n}{\omega_g E_n^2} \tag{7}$$

where ω_g is the grid frequency, and E_n the base voltage. Thus, unlike the inductors, the filter capacitor is proportional to the nominal power of the inverter [7].

In this paper, the LCL filter of the first two inverters are designed considering that one inverter has a 30 percent higher rated power than the other while keeping all other parameters the same. It is important to mention that while the LCL filter parameters were selected using this method, the analytical framework developed in Section III is still valid for any values of the LCL filter parameters.

C. Multiple Resonances Peaks

Similar to the case with identical LCL filters, the addition of parallel inverters changes the frequency response of the system [8-9]. Fig. 3 illustrates the positions of the resonance peaks with two grid-connected inverters with LCL filters values given by Table I.

To compare with the case of identical inverters, Fig. 3 also shows the resonance peaks of two more cases: one with two identical inverters with the parameters of inverter A (Fig. 4(a)), and another one with the parameters of inverter B (Fig. 4(b)). For the three cases, the position of the LCL filter main resonance remains the same at

$$\omega_{res} = \sqrt{(L_{11}+L_{21})/(L_{11}L_{21}C_{f1})}. \tag{8}$$

For the case of two different LCL filters, however, the frequency of the second resonance is given by:

TABLE I

SYSTEM PARAMETERS

Inverter Parameters		
	Inverter A	Inverter B
Power rating	P_{n1}=2 MVA	P_{n2}=1.4 MVA
Voltage rating	480 V	480 V
Inverter-side inductance	L_{11}=20 μH	L_{12}=28 μH
Grid-side indutance	L_{21}=12.2 μH	L_{22}=17.1 μH
Filter capacitor	C_{f1}=Δ3x480 μF	C_{f2}=Δ3x343 μF
Proportional gain	0.125	0.155
Sampling frequency	4 kHz	4 kHz
Switching frequency	4 kHz	4 kHz
Grid Inductance	L_g=10 μH	

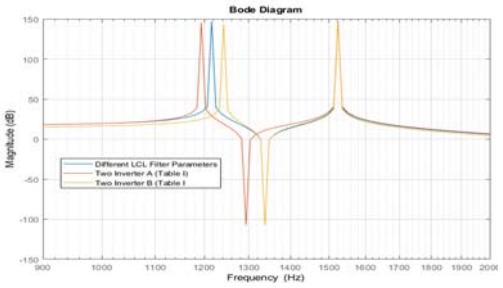

Fig. 3. Resonance peaks of the paralleled grid-connected inverters.

$$\omega_{res2} = \sqrt{\frac{(L_{11}+(L_{21}+(1+n')L_g)}{(L_{11}(L_{21}+(1+n')L_g)C_{f1})}}, \quad (9)$$

$$= \sqrt{\frac{(L_{12}+(L_{22}+(1+(1/n'))L_g)}{(L_{12}(L_{22}+(1+(1/n'))L_g)C_{f2})}} \quad (10)$$

where n' is a gain given by the ratio of the power ratings of the inverters; that is,

$$n' = P_{n2} / P_{n1}. \quad (11)$$

III. Stability Analysis Of the Paralleled Inverters

A. Control Strategy

The block diagram of the multiple input, multiple output (MIMO) current-control loop in the s-domain for the two paralleled grid-connected inverter from Fig. 1 is presented in Fig. 5(a). In the figure, $\mathbf{i_{nref}}$ is the reference commands for the grid-side current given to the controllers, $\mathbf{G_{d\_DSP}(s)}$ the diagonal transfer function which accounts for the delays of the system and $\mathbf{G_{PI}(s)}$ is a diagonal matrix that contains the controller of each inverter which is chosen in this paper as follows:

$$\mathbf{G_{PI}(s)} = \begin{bmatrix} PI_1 & 0 \\ 0 & PI_2 \end{bmatrix}, \quad PI_{1,2}(s) = K_P + \frac{K_i}{s}. \quad (12)$$

Although the system can be analyzed in the s-domain as in [10], the z-domain modeling of the system will be considered in this paper since the inverters are usually digitally controlled with a microcontroller. Thus, the discrete representation of the controller from Fig. 5(a) is presented in Fig. 5(b), where the PI controller and the transfer function matrix were discretized by using a Tustin and zero-order-hold (ZOH) transform, respectively [11]. Moreover, $\mathbf{G_{PI}'(z)}$ now contains both the PI controllers of the inverters as well as the system delays.

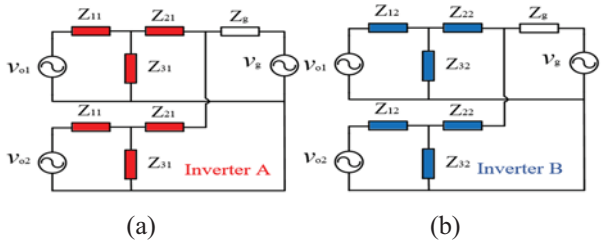

Fig. 4. Schematic of two paralleled grid-connected inverters with the LCL parameters of (a) inverterter A, (b) inverter B.

B. Stability Analysis for Grid-Side Current

The stability of the system can be analyzed by examining the poles of the multivariable system [8]. From Fig. 5(b), the closed-loop transfer function of the multivariable system can be derived as follows:

$$\begin{bmatrix} i_{o1} \\ i_{o2} \end{bmatrix} = \begin{bmatrix} T_{11} & T_{12} \\ T_{21} & T_{22} \end{bmatrix} \cdot \begin{bmatrix} i_{1ref} \\ i_{2ref} \end{bmatrix}, \quad (13)$$

$$\mathbf{T(z)} = [\mathbf{I} + \mathbf{G(z)PI'(z)}]^{-1} \cdot [\mathbf{G(z)PI'(z)}]. \quad (14)$$

where $\mathbf{I}$ represents the identity matrix. From (14), the diagonal element T_{11}, and the non-diagonal element T_{12} are derived as follows:

$$T_{11} = \frac{i_{o1}}{i_{1ref}} = \frac{G_{11}PI_1' + (PI_1'PI_2')(G_{11}G_{22} - G_{12}G_{21})}{(1+G_{11}PI_1')(1+G_{22}PI_2') - (G_{12}PI_2')(G_{21}PI_1')} \quad (15)$$

$$T_{12} = \frac{i_{o1}}{i_{2ref}} = \frac{G_{12}PI_2'}{(1+G_{11}PI_1')(1+G_{22}PI_2') - (G_{12}PI_2')(G_{21}PI_1')} \quad (16)$$

The other elements of the $\mathbf{T(z)}$ matrix are given in the Appendix. Expressions (15)-(16) show that the denominators of the system are identical since the poles of a multivariable system have to be the same [10]. Thus, the characteristic equation of the system is:

$$(1+G_{11}PI_1')(1+G_{22}PI_2') - (G_{12}PI_2')(G_{21}PI_1') = 0. \quad (17)$$

From (17), it is clear that the system stability depends on both controllers as well as the four elements of the transfer function matrix $\mathbf{G(z)}$. Then, if and only if all the poles from (14) are inside of the unit circle, the system will be stable.

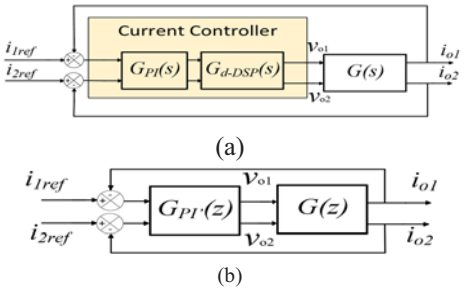

Fig. 5. Multiple current-control loop for the grid-side currents in (a) s-domain, (b) z-domain.

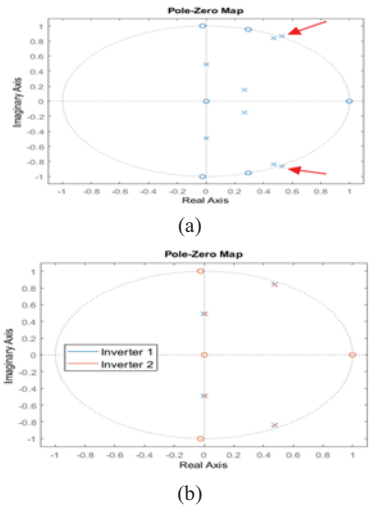

Fig. 6. Poles of the (a) paralleled inverter system with Kp from Table I, (b) individual inverter system.

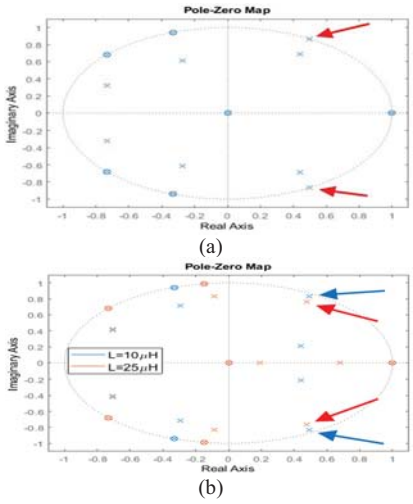

Fig. 7. Poles of the system for (a) maximum value of Kp for the interative stability, (b) inversely changing the value of Kp for the two inverters.

Therefore, proper selection of the proportional gains of the current controllers will determine the stability of the system.

The poles of the system are plotted in Fig. 6(a) using the parameters from Table I and (17). However, the system will be unstable since some of the poles are outside of the unit circle. The significance of this result is that the proportional gains were selected without considering the coupling of the inverters, such that the inverters were stable when they were individually connected to the grid, as seen in Fig. 6(b). Thus, despite the inverters being stable individually with these gains, they become unstable once they are connected to the grid due to mutual coupling. This means that conventional current controller design for individual inverters might not be sufficient to guarantee the stability of multiple grid-connected inverters with different LCL filters.

IV. Comparison with the Stability Analysis of Identical LCL filters

A. Motivation for Comparison

While the previous analysis allows one to accurately determine the stability of the system, the downside is that the analysis becomes more complicated once more inverters are added to microgrid. This section will show that the regions of stability of the inverters with different LCL filter parameters have some similarities and differences with the case when all paralleled inverters have the same LCL filter values. Understanding these similarities will allow the simplification of the stability analysis of a system with different LCL filters.

For multiple grid-connected inverters with the same LCL filter, [8] showed that the grid-side current is comprised of a current that circulates between two inverters (i.e., interactive current) and one that is injected into the grid ((i.e., common current). Then, the stability of the system can be determined by performing single-input, single-output (SISO) analysis techniques (e.g., root locus) to the open-loop forward path of the closed-loop transfer function of the interactive and common currents [8]. Then, the overall system will only be stable if it has interactive- and common-current stability [8-9].

The analysis method described in [8] will be applied to the circuit in Fig. 1 to calculate the stability range of Kp for the common and interactive currents. To do so, the circuit in Fig. 1 will be reconfigured as the two circuits from Fig. 4. Fig. 4(a) shows the equivalent model of the system that only has two inverters A connected to the grid while Fig. 4(b) has two inverters B connected. Then, the stability analysis in [8] will be implemented to the independent circuits to obtain their values of Kp for the interactive- and common-current stability. The stability ranges of the two inverters are calculated and presented in Table II. Now the values of Kp in Table II can be tested in the characteristic equation of (17) to determine similarities and differences between the analysis of identical and different LCL filters.

B. Interactive-Current Stability

The maximum values of Kp for the interactive-current stability of both inverters play an important role in the system stability with different LCL filter parameters. In this case, selecting the maximum values of Kp for the interactive-current stability of both inverters result in the poles of the system being exactly on the edge of the unit circle as shown in Fig. 7(a). Moreover, the positions of these poles with these values of Kp do not change significantly with changes in the grid inductance which is similar to the behavior of the interactive-current stability in [8]. However, this behavior occurs mainly when the proportional gain of both inverters are selected close to maximum Kp for the interactive-current stability. If one of the inverters is selected with a proportional gain lower than its maximum interactive-current stability gain, the other inverter can increase its proportional gain Kp higher than its maximum value for the interactive-current stability. This is presented in Fig. 7(b) where although the value of Kp for the first inverter was selected higher than its interactive-current stability range at 0.125, the poles of the system remain inside of the unit circle due to reducing the gain of the second inverter to 0.07.

TABLE II

STABILITY RANGE

Stability Range for Proportional Gain K_P		
Inverters	Inverter A	Inverter B
Interactive Stability	$0< K_P<0.116$	$0<K_P <0.162$
Common Stability	$0<K_P <0.158$	$0< K_P<0.205$

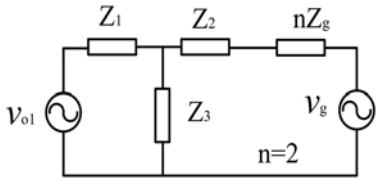

Fig. 8. Equivalent N-inverter model to measure the common-current stability gains.

However, changes to the grid inductance with these values of Kp, will change the position of the poles of the system, as seen in Fig 7(b).

C. *Common-Current Stability*

Similarly, the maximum value of Kp for the common currents of the inverters will also play an important role in the stability of the system with different LCL filters. To calculate the range of stability of the common currents, the N-equivalent model of the inverters will be used as in [8,10]. In this model, an inverter "perceives" the grid inductance N times bigger, as illustrated in Fig. 8 [10]. It is important to mention that this model is only valid for the analysis when inverter A and inverter B have a 1:1 ratio. Using this model, the common-current stability for the system in Fig. 4(a) and Fig. 4(b) is calculated and presented in Table II. However, since the values of Kp for the common-current stability are larger than the values of the interactive-current stability, the common stability cannot be tested using the parameters from Table I. That is, if the inverters are commonly unstable, they will also be interactively unstable.

Thus, the filter values of inverters A and B are replaced by the values of inverters C and D from Table III to verify the effect of the common-current stability for inverters with different LCL filters. Using these filter parameters allows the system to have a stability case where the inverters can be commonly unstable but interactively stable. Then, following the same methods as before, the ranges of Kp for the interactive- and common-current stability are calculated and presented in Table III. In this case, selecting the maximum values of Kp for the common-current stability using the N-equivalent model results in the poles of the system being exactly on the edge of the unit circle, as shown in Fig. 9.

The results from this section show that the interactive and common stability analysis techniques implemented in [8] can be used to determine the stability ranges of the proportional gain of inverters with different LCL filters that have some variations in their power ratings. The main modification that needs to be made is that the system with different inverters needs to be converted into multiple systems with identical LCL filters as presented in Fig. 4.

TABLE III

SYSTEM PARAMETERS TO TEST COMMON STABILIY

Inverter Parameters		
	Inverter C	Inverter D
Power rating	P_{n1}=0.75 MVA	P_{n2}=0.54 MVA
Inverter-side inductance	L_{11}=110 µH	L_{12}=154 µH
Grid-side indutance	L_{21}=12.2 µH	L_{22}=17.1 µH
Filter capacitor	C_{f11}=Δ3x600 µF	C_{f12}=Δ3x428 µF
Interactive Stability	$0<K_P <0.352$	$0<K_P <0.492$
Common Stability	$0<K_P <0.132$	$0<K_P <0.274$
Grid Inductance	L_g=10 µH	

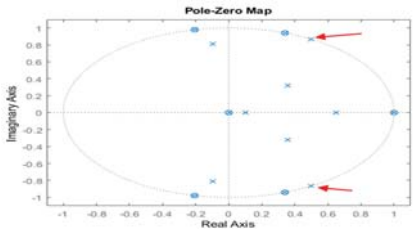

Fig. 9. Poles of the system for maximum values of Kp for the common-current stability in Table III.

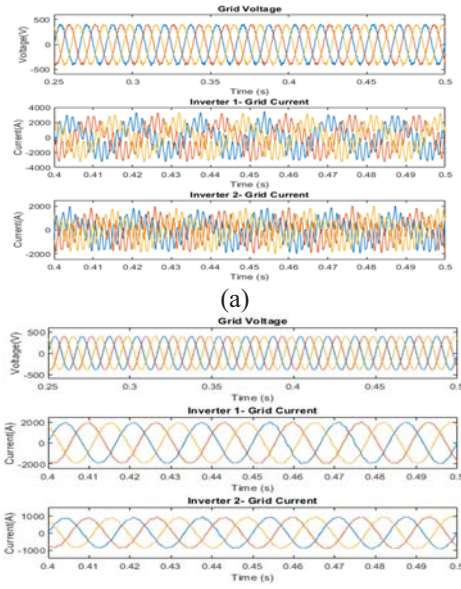

Fig. 10. Simulation results of (a) multiple paralleled- (b) individual grid-connected inverters with the values from Table I.

Then, the method in [8] can be applied to each of those equivalent circuits to obtain the maximum value of the proportional gains for the interactive- and common-current stability. Finally, the value of Kp of each inverter needs to be lower than the maximum interactive- and common-current stability gains.

V. Simulation Results

In order to validate the theoretical analysis from the previous section, MATLAB/SIMULINK™ is used to model a system consisting of two grid-connected inverters with the parameters from Table I. Inverter A and inverter B are given a reference

current of 2 kA and 1 kA, respectively, that needs to be tracked with the current controllers. Fig. 10(a) shows that the current controller of the inverters does not track the reference currents and produces harmonics and distortion on the grid current and voltage. This occurs since the poles of the system were outside of the unit circle as shown in Fig. 6(a), making the system unstable. Similarly, Fig. 10(b) shows that when only one of the inverters is connected to the grid at a time, the current controller can properly track its reference current without great distortion. This is the result of the poles of the system being inside of the unit circle in Fig. 6(b), making the system stable.

VI. Conclusion

The modeling and stability analysis for two paralleled grid-connected inverters with different LCL filters using the grid-side current as feedback was performed. The importance of properly selecting the proportional gains of the current controllers using this model was shown since individually stable inverters can become unstable when connected in parallel because of the effect of the grid inductance. The results from this paper indicated that a method similar to the interactive- and common-current analysis technique used to determine the stability ranges of inverters with identical LCL filers can be implemented on a system with different LCL filer parameters to get a good approximation on the maximum values of the inverters' current controller gains without having to derive the equations of the MIMO system. However, the MIMO model for the plant could be derived if a more accurate result is needed using the method described in this paper to guarantee the stability of the system. Finally, the theoretical analysis was validated through simulations.

Appendix

$$G_{22} = \frac{i_{o2}}{v_{o2}} = \frac{Z_{31}}{(Z_{12}+Z_{32})(Z_B + \dfrac{Z_g Z_A}{(Z_g+Z_A)})}$$

$$G_{21} = \frac{i_{o2}}{v_{o1}} = -\frac{Z_{31}Z_g}{(Z_{11}+Z_{31})(Z_B + \dfrac{Z_g Z_A}{(Z_g+Z_A)})(Z_g+Z_A)}$$

$$T_{22} = \frac{i_{o2}}{i_{2ref}} = \frac{G_{22}PI_2^{'} + (PI_1^{'}PI_2^{'})(G_{11}G_{22}-G_{12}G_{21})}{(1+G_{11}PI_1^{'})(1+G_{22}PI_2^{'}) - (G_{12}PI_2^{'})(G_{21}PI_1^{'})}$$

$$T_{21} = \frac{i_{o2}}{i_{1ref}} = \frac{G_{21}PI_1^{'}}{(1+G_{11}PI_1^{'})(1+G_{22}PI_2^{'}) - (G_{12}PI_2^{'})(G_{21}PI_1^{'})}$$

Acknowledgments

The authors are grateful to the financial support from the NSF I/UCRC Grid-Connected Advanced Power Electronic Systems (GRAPES) under grant IIP-1439700.

References

[1] M. Lu, X. Wang, F. Blaabjerg and P. C. Loh, "An analysis method for harmonic resonance and stability of multi-paralleled LCL-filtered inverters," *2015 IEEE 6th International Symposium on Power Electronics for Distributed Generation Systems (PEDG)*, Aachen, 2015, pp. 1-6, doi: 10.1109/PEDG.2015.7223086.

[2] J. H. R. Enslin and P. J. M. Heskes, "Harmonic interaction between a large number of distributed power inverters and the distribution network," *IEEE 34th Annual Conference on Power Electronics Specialist, 2003. PESC '03*, Acapulco, Mexico, 2003, pp. 1742-1747 vol. 4, doi: 10.1109/PESC.2003.1217719.

[3] M. Lu, X. Wang, P. C. Loh and F. Blaabjerg, "Resonance Interaction of Multiparallel Grid-Connected Inverters With LCL Filter," *IEEE Transactions on Power Electronics*, vol. 32, no. 2, pp. 894-899, Feb. 2017, doi: 10.1109/TPEL.2016.2585547.

[4] J. He, Y. W. Li, D. Bosnjak and B. Harris, "Investigation and Active Damping of Multiple Resonances in a Parallel-Inverter-Based Microgrid," *IEEE Transactions on Power Electronics*, vol. 28, no. 1, pp. 234-246, Jan. 2013,doi: 10.1109/TPEL.2012.2195032.

[5] F. Cavazzana, P. Mattavelli, M. Corradin and I. Toigo, "On the stability analysis of multiple parallel inverters using the impedance multiplication effect," *8th IET International Conference on Power Electronics, Machines and Drives (PEMD 2016)*, Glasgow, 2016, pp. 1-6, doi: 10.1049/cp.2016.0213.

[6] H. Wei, S. Jianjun, M. Qian, Y. Chenxu, L. Fei and Z. Xiaoming, "Modeling and resonant characteristics analysis of multiple paralleled grid-connected inverters with LCL filter," *2014 IEEE Energy Conversion Congress and Exposition (ECCE)*, Pittsburgh, PA, 2014, pp. 3371-3377, doi: 10.1109/ECCE.2014.6953858.

[7] A. Reznik, M. G. Simões, A. Al-Durra and S. M. Muyeen, "LCL Filter Design and Performance Analysis for Grid-Interconnected Systems," *IEEE Transactions on Industry Applications*, vol. 50, no. 2, pp. 1225-1232, March-April 2014, doi: 10.1109/TIA.2013.2274612.

[8] M. Lu, X. Wang, P. C. Loh and F. Blaabjerg, "Resonance Interaction of Multiparallel Grid-Connected Inverters With LCL Filter," *IEEE Transactions on Power Electronics*, vol. 32, no. 2, pp. 894-899, Feb. 2017, doi: 10.1109/TPEL.2016.2585547.

[9] M. Lu, X. Wang, P. C. Loh and F. Blaabjerg, "Interaction and aggregated modeling of multiple paralleled inverters with LCL filter," *2015 IEEE Energy Conversion Congress and Exposition (ECCE)*, Montreal, QC, 2015, pp. 1954-1959, doi: 10.1109/ECCE.2015.7309936.

[10] J. L. Agorreta, M. Borrega, J. López and L. Marroyo, "Modeling and Control of N -Paralleled Grid-Connected Inverters With LCL Filter Coupled Due to Grid Impedance in PV Plants," *IEEE Transactions on Power Electronics*, vol. 26, no. 3, pp. 770-785, March 2011, doi: 10.1109/TPEL.2010.2095429.

[11] S. G. Parker, B. P. McGrath and D. G. Holmes, "Regions of Active Damping Control for LCL Filters," *IEEE Transactions on Industry Applications*, vol. 50, no. 1, pp. 424-432, Jan.-Feb. 2014, doi: 10.1109/TIA.2013.2266892.